Ultrastructure and estimation of element of tissue of each the parotid, submandibular and sublingual gland of domestic rabbit in Iraq.

Wafaa H. AL-Hashemi[1], Mohummed E. mansur[2]

[1]*Lecturer, M.SC., Basic Science Department , College of Dentistry, University of Kufa/Iraq.*
[2]*Assis prof, Phd, Science Department, College of science, University of Kufa/Iraq.*

Abstract:

Introduction: The little attention of estimation the element not in saliva but in the tissue of salivary glands, will estimation it by mapping analysis. As well as, the mapping arranged of salivon in scanning electron microscope.

Material and methods: use scanning electron microscope and Energy dispersing X-ray spectroscope (EDS).

Results: estimation the elements in the tissue of major salivary gland, inspect the significant (P≤0.05) of concentration the carbon electrolyte in the parotid gland tissue comparative with the submandibular and sublingual gland respectively. Expound the significant (P≤0.05) of concentration the sodium, calcium and sulfate element in the submandibular gland tissue comparative with the sublingual and parotid gland respectively. Also, represent the significant (P≤0.05) of concentration the potassium and iodine element in the submandibular gland tissue comparative with the parotid and sublingual gland respectively. Also, clarify the significant (P≤0.05) of concentration the phosphate electrolyte in the sublingual gland tissue comparative with the submandibular and parotid gland respectively. The ultrastructure of the parotid gland seem three dimension under the scanning electron microscope, The collagen fiber in inter-lober connective tissue that found in parotid gland very thick than the other major salivary gland, Expound that the serous cells are pyramidal in shape illustrate the outer surface is not smooth contain abundant alveolar invaginations in areas that observed in SEM. In submandibular that shown cells in the serous tubules are pyramidal shape and larger than one layer of cuboidal cells in the intercalated duct. In that, the serous cells are arranged one each other that formed tubule structure, its rounded by MECs. The MECs under SEM detail's the MECs have few primary cytoplasmic processes that longer and thinner primary cytoplasmic processes and in free end are few branching final cytoplasmic processes, And the some primary cytoplasmic processes are extending in to other cell in same acini or along serous tubules and intercalated duct, Often these MECs have three and some MECs have four primary cytoplasmic processes that found around serous tubules and intercalated ducts. Whereas the MECs have five, six and some MECs have four primary cytoplasmic processes are shorter, and thicker primary cytoplasmic processes were send the final cytoplasmic processes were large in numbers and formed around cells always, mucous cells. Ultrastructure of sublingual gland expound the serous cell smaller in size than he mucous cell underling also the mucous acini are elongated and catching by MEC are extending their primary cytoplasmic processing on mucous cell and plug in terminal ending that sending many final cytoplasmic processing, also each branch are forming plug.

Conclusion: deduction the deference of the structure and elements component of tissue in each parotid, submandibular and sublingual glands.

INTRODUCTION:

The salivary gland is exocrine gland it is consider the gate of the digestive system. The salivary gland Saliva acting a major starring role in scheme of the buccal cavity, digestion, and lubrication. (Lamy, Capela-Silva and Tvarijonaviciute, 2018)

The salivary glands are essential for the maintenance of the buccal cavity homeostasis. Salivary glands are fundamental organs that create and discharge saliva to the oral cavity of the all mammlian (Junqueria and Carneiro, 2013; Paula *et al*., 2017; Cruchley and Bergmeier, 2018).

Salivary produced saliva spit for kept damp oral cavity. That become thin of layer liquid, which covered mucosa and teeth. Spit is complex fluid. The most critical capacity for keep up prosperity of mouth. (Proctor and Carpenter, 2014).

The acini of major salivary gland will divide according structure and secreting nature. (One) serous acini are generally, contain semispherical granules with watery protein emission (zymogen) (constitute glycosylated or non-glycosylated) and discharge by exocytosis. (Two) mucous acini supply a viscosity; foul glycoprotein (mucin) inclosing by granules in apical cytoplasm of mucous cells.

(Third) Blended, or seromucous, acini contain segments of the two kinds, yet one sort of the secretory unit that is knowledge. The mixed secretory units are normally seen as serous demilunes (half-moons like) arcs on mucous acini. Myoepithelial cells are likewise, seen around acini and intercalated ducts, yet here they are more axle formed (Nanci, 2012; Cruchley and Bergmeier, 2018).

The secretory end-piece (acini or tubulo-alveolar) beginning the secretory fluid pass cross small canaliculi into the intercalated ducts, that drain their secretion into the striated ducts then drain into execratory ducts. A sporadic myoepithelial cell layer fixed with cuboidal epithelium rounds intercalated ducts. Striated duct are recognizing by basal striations of columnar epithelium. (Paula *et al.,* 2017). The main excretory ducts were assigned initially as Stensen's duct, Wharton's duct, Bartholin's duct in place of parotid, submandibular, and sublingual gland respectively (Tandler *et al*., 2001). A single secretory unite named salivon, which composed of the end-pieces acinus, intercalated duct and striated duct (Patterson *et al.,* 2012; Buseth and Saunders, 2014; Alvarez-Castaneda, Alvarez, and Gonzalez-Ruiz, 2017).

Changes the saliva component in glandular ductal cells: Saliva is isotonic that secreted by acinar cells and flow across the ductal system when the saliva reach the striated duct lumen, the ductal cells are removed the sodium chloride, the saliva become hypotonic. The changes of sodium chloride concentration is related with the salivary flow rate; when elevated its have a great sodium chloride concentration (Segawa *et al.*, 2000; Brini and Carafoli, 2011). The removal of salt by ductal cells is dependent upon the Na+ by the Na+ / K+ pumps, really, the striated duct cells have numerous of basolateral located ATP-generating mitochondria, for a high sodium chloride concentration that secretion. (Roussa, 2011; Ambudkar, 2014). Membrane transporting proteins that expel chloride from ductal lumen into the interstitial tissue around ductal wall (Ohtomo *et al.,* 2011). Bicarbonate compound are imperative component of saliva that increase alkaloid when increase flow rate for avoiding dissolution of "tooth mineral" (Romanenko *et al*, 2010; Proctor, 2016).

Aim is to studies of intra-comparative among parotid, submandibular as well as sublingual glands of normal domestic rabbit in Iraq by study the Ultrastructure of each gland and estimation of electrolytes carbon, Iodide, Sodium, potassium calcium, phosphate, sulfate and oxygen.

MATERIAL AND METHODS:

The estimation the electrolyte carbon, Iodide, Sodium, potassium calcium, phosphate, sulfate and oxygen in the major salivary gland tissue: same procedure until blacking the sample of tissue then supplies energy dispersion X-ray spectroscope (EDS) that show the spectrum and atom weight and mapping analysis of all elements. The measure of elements in the (EDS) that give really concentration of the each element in the tissue. The supplies energy dispersion X-ray spectroscope (EDS) in the SEM and show the spectrum and mapping analysis in the software. There are use sixtey adult males domestic rabbit that perpetration of the tissue they excretion all saliva from the ductal system for measure the electrolyte only in tissue.

Electron Microscope:

Scanning Electron Microscope SEM: there are use sixtey adult males domestic rabbit. Preparing tissue for the SEM. The preparation of tissue: after enthusiasm the animal become ejection the normal saline in the jugular vein for keep out all blood from the blood vessel stopped until all the blood are removal then become essay obtain the glands from the animal and sculpture it.

Fixation: Prepare fixative solution and fill the scintillation vials with fixative. Fixative 2.5ml glutaraldehyde and 2.5ml formalied procedures to better differentiate connective tissue components.

Osmium Tetroxide Step:

Solution prepared by dissolved 0.5 gram capsules in 25 mLs of water in dark conteners the concentration of solution about 2% solution. Let solution sit at 20 C. Take 1ml the osmium tetroxide solution S4O4 from dark ampules dilute by 3 ml of phosphate buffer 25Mm. The solution are colorless when taken gray color the solution are inactive. Can be stored several days in the cold apartment to become black.

Drain the osmium solution by micropipette and washing the blacken tissue by 25mm PB.

Change the container of tissue into plastic Eppendorf then use 30% alcohol 3 time each one 5 min. and drain alcohol and add BP. Add 50% alcohol 3 time each one 5 min, then series alcohol 70%, 75% , 90%, 100%.

Drying the tissue Placed the blacked tissue in the Eppendorf with 70%, then drier its by instrument Critical point dryer. Next, covered the sample with gold by sputter coating. Finally, exam the sample in SEM.

RESULTS

The estimation the electrolyte carbon, Iodide, Sodium, potassium calcium, phosphate, sulfate and oxygen in the major salivary gland tissue:

In current study measured the element in the tissue of major salivary gland before measure it the tissue treated by osmium until the tissue black color for they excretion all saliva from the ductal system for measure the electrolyte only in tissue. That use the Energy dispersing X-ray spectroscope (EDS), the mapping analysis that exhibit the found and distribution of each element of in the parotid, submandibular and sublingual tissue. The procedure for perpetration of tissue that use osmium, yttrium and zinc befor applied EDS on tissue. The result in table the osmium and zinc were excluded from the Data table as they are using in tissue preparation. In table (1) Inspect the significant (P≤0.05) of concentration the carbon electrolyte in tissue of the parotid gland tissue comparative with the submandibular then sublingual gland respectively. In same table expound the significant (P≤0.05) of concentration the sodium electrolyte in the submandibular Likewise, represent the significant (P≤0.05) of concentration the sulfate electrolyte in the submandibular gland tissue comparative with the sublingual and parotid gland respectively.

As well, clarify the significant (P≤0.05) of concentration the iodine electrolyte in the submandibular gland tissue comparative with the parotid and sublingual gland respectively.

Furthermore, expound the significant (P≤0.05) of concentration the sulfate electrolyte in the submandibular gland tissue comparative with the sublingual and parotid gland respectively, gland tissue comparative with the sublingual and parotid gland respectively. Also, represent the significant (P≤0.05) of concentration the potassium electrolyte in the submandibular gland tissue comparative with the parotid and sublingual gland respectively. Clarify the significant (P≤0.05) of concentration the calcium electrolyte in the submandibulargland tissue comparative with the sublingual and parotid gland respectively. Also, clarify the significant (P≤0.05) of in the concentration the phosphate electrolyte sublingual gland tissue comparative with the submandibular and parotid gland respectively.

Table (1): the estimation the electrolyte carbon, Iodide, Sodium, potassium calcium, phosphate, sulfate and oxygen in the major salivary gland tissue.

n = 10 / NO.	the electrolyte of major salivary glands tissue	The Parotid gland Mean ± SD	The Submandibular gland Mean ± SD	The Sublingual gland Mean ± SD
1	carbon	75.8480 ± 0.80723*	54.4200 ± 0.94520**	52.1370 ± 0.91747***
2	sodium	0.4010 ± 0.00876*	0.8640 ± 0.0043**	0.4880 ± 0.08892***
3	potassium	0.3380 ± 0.01317*	0.6360 ± 0.01075**	0.2430 ± 0.0082***
4	calcium	0.5170 ± 0.01636*	0.9810 ± 0.00876**	0.6650 ± 0.01581***
5	phosphate	0.6040 ± 0.01578*	0.6180 ± 0.01033**	0.6300 ± 0.00756***
6	sulfate	0.2610 ± 0.00876*	0.6380 ± 0.01814**	0.4690 ± 0.00876***
7	Iodine	1.5680 ± 0.41587*	1.9650 ± 0.01269**	0.8910 ± 0.01370***
8	oxygen	23.1360 ± 0.29376*	26.3640 ± 0.77595**	24.3660 ± 1.18347***

* indicate significant (P≤0.05) between Parotid and submandibular, ** represent significant (P≤0.05) between submandibular and sublingual, *** Clarify significant (P≤0.05) between Parotid and sublingul gland.
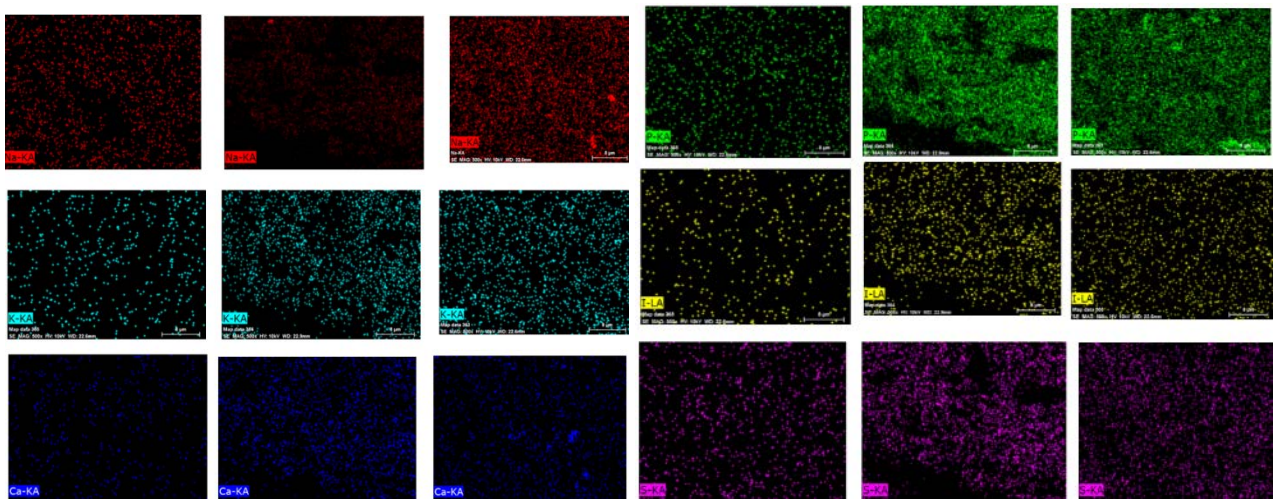

Figure (1): Showing-mapping analysis in EDS each element carbon, Iodide, Sodium, potassium calcium, phosphate, sulfate and oxygen in the major salivary gland. The left image of parotid gland the meddle image for submandibular gland the right image for sublingual gland
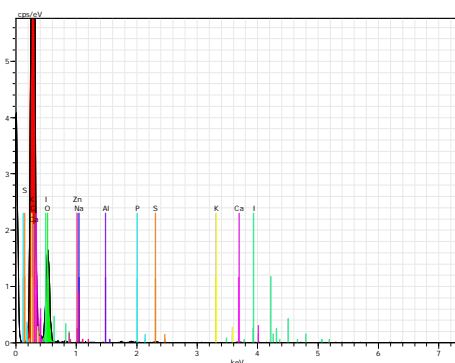

Figure (2): Spectrum of EDS mapping analysis of the elements of the elements that found in parotid gland.
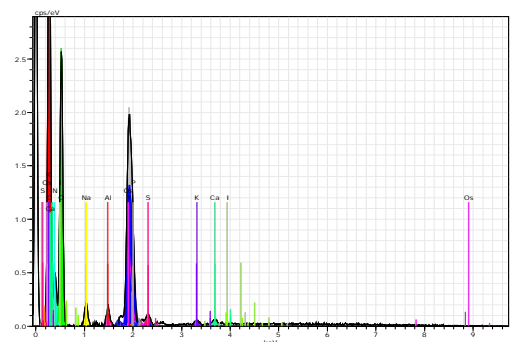

Figure (3): Spectrum of EDS mapping analysis of the elements of the elements that found in submandibular gland.
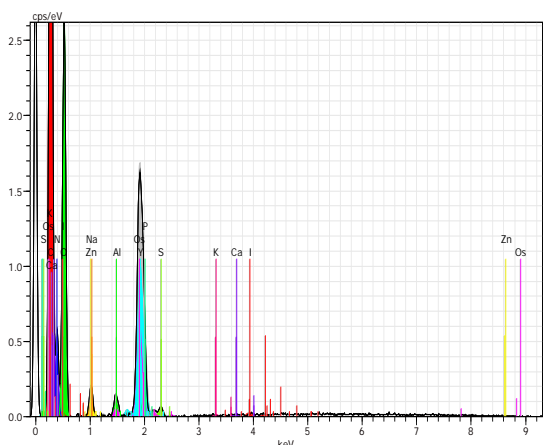
Figure (4): Spectrum of EDS mapping analysis of the elements of the elements that found in sublingual gland.

Ultrastructure of Myoepithelial cell in major salivary gland indicated under scanning electron microscope (SEM).

The myoepithelial cell have many primary cytoplasmic processing. In SEM revealed that MEC processes ramify into numerous secondary and tertiary divisions that called final cytoplasmic processing. There can be up to thirty terminal processes extending from each MEC that expound in fig (21). The average number of final cytoplasmic processing extending from the MECs that have four, five, six primary cytoplasmic processing is more than the MECs have three primary cytoplasmic processing (that see in scanning electron microscope). It is also noted that the thicker primary cytoplasmic processes occur in the MECs that have four, five, six primary cytoplasmic processing than the MECs have three primary cytoplasmic processing, that clarify in figure (19, 20, 21, 22).

The MECs under SEM detail's the MECs have few primary cytoplasmic processes that longer and thinner primary cytoplasmic processes and in free end are few branching final cytoplasmic processes, And the some primary cytoplasmic processes are extending in to other cell in same acini or along serous tubules and intercalated duct, that show Figure (20). Often these MECs have three or four primary cytoplasmic processes that found around serous tubules and intercalated duct. Whereas the MECs have five, six primary cytoplasmic processes are shorter, and thicker primary cytoplasmic processes the free end are forming plug and then forming final cytoplasmic processes. The final cytoplasmic processes are large in numbers and formed around cells always, mucous cells that expound in the figure (19).

Ultrastructure of parotid gland:

The parotid gland seem under the scanning electron microscope when fixative in kwanovisky fixative then reduced by osmium tetroxide. three-dimensional network of dense regular inter-lobar connective-tissue collagen fibers. The collagen fiber in inter-lober connective tissue that found in parotid gland very thick than the other major salivary gland, clarify in figure (5 , 6, 7 and 8).

Additionally, coarser bundles of collagen fibers traversing the intra-lobular spaces and linking neighboring acini. At

high striated ducts embedded in the connective-tissue septa can be observed in the figure (9)

Each lobule was surrounded by a dense network of collagen fiber in inter-lober connective tissue, that appeared to be continuous with the interacinar connective-tissue stroma, that clarify in figure (3, 4, 5) the acini seem embedding in collagen fiber in inter-lober connective tissue.

In the figure (11) that clarify the lobules of parotid gland contain serous cells and observed cross section of intercalated ducts among them. Also observed many striated duct arranged in postulated structure additionally shown collagen fibers among them.

In the figure (12) clarify clearly the striated duct. The surface of the striated duct are longitudinal threat like structure. In the figure (13) expound serous cells are pyramidal in shape and very small in size under SEM 100nm.

In the figure (14, 15) illustrate the outer surface is not smooth contain abundant alveolar invaginations in areas that observed in SEM.
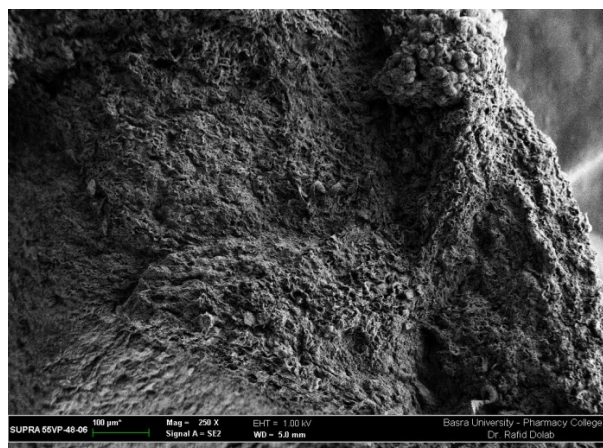

Figure (5): showing histological section of parotid gland, 3-dimensional of connective tissue fibers. The collagen fiber in inter-lober connective tissue, the serous acini and the striated duct 100µm
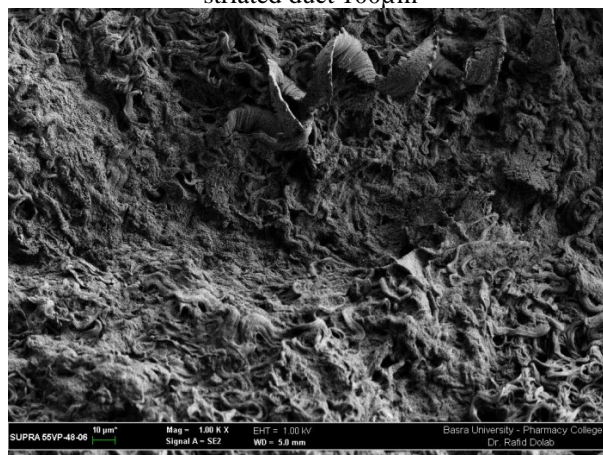

Figure (6): showing histological section of parotid gland, network of connective tissue of collagen fibers, the collagen fiber in inter-lober connective tissue 10µm.

Figure (7): showing histological section of parotid gland, 3D network of connective tissue of collagen fibers The collagen fiber in inter-lober connective tissue 10µm
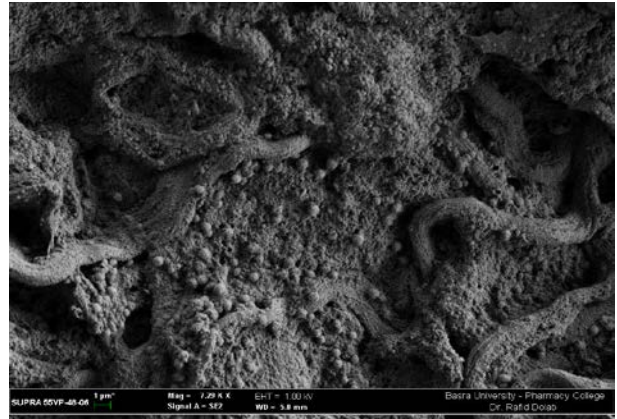

Figure (10): showing histological section of parotid gland, showing the serous acini and the striated duct 1µm
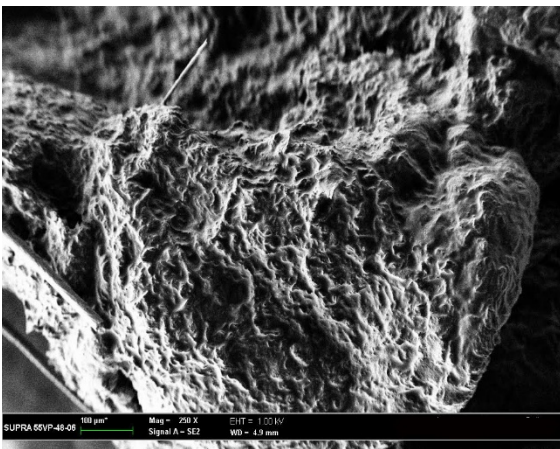

Figure (8): showing histological section of parotid gland, the collagen fiber in inter-lober connective tissue 100µm.
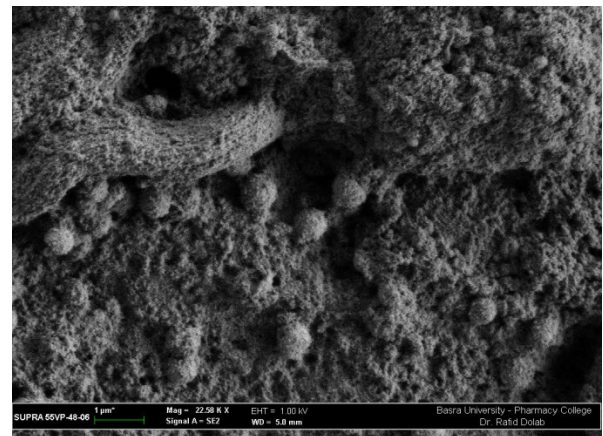

Figure (11): showing histological section of parotid gland, showing the serous acini and the striated duct 1µm
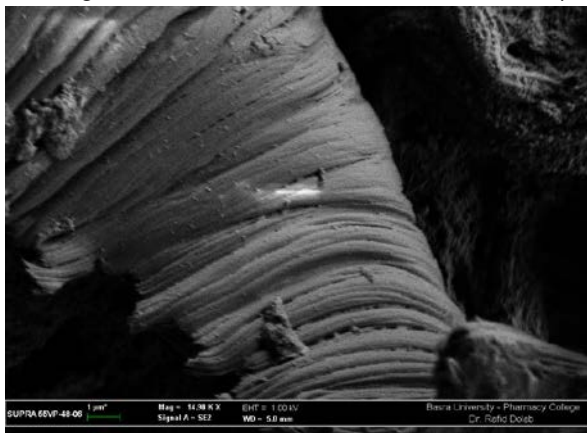

Fig (9) showing histological section of parotid gland, the collagen fiber in inter-lober connective tissue 1µm.
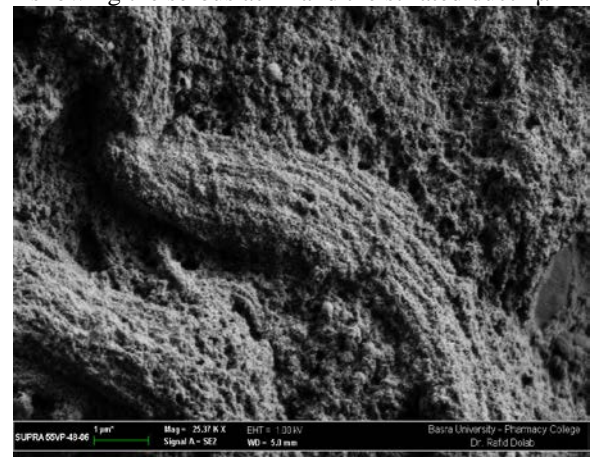

Figure (12): showing histological section of parotid gland, A three-dimensional supporting inter-lobar connective-tissue network is observed with bundles of collagen fibrils spanning. Intra-lober duct 1µm
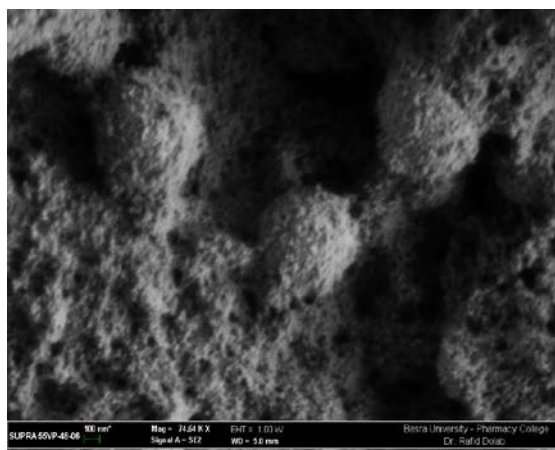
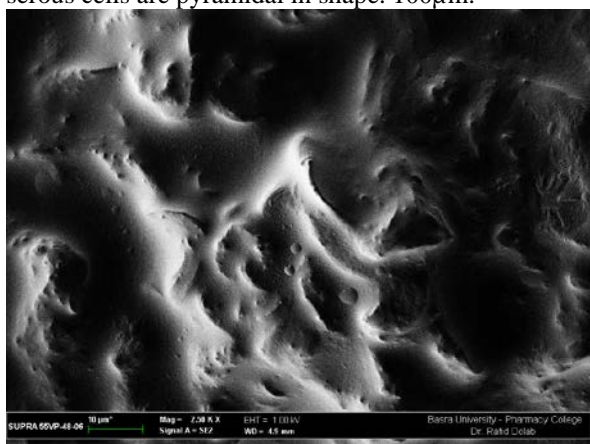Figure (13) showing histological section of parotid gland, serous cells are pyramidal in shape. 100µm.

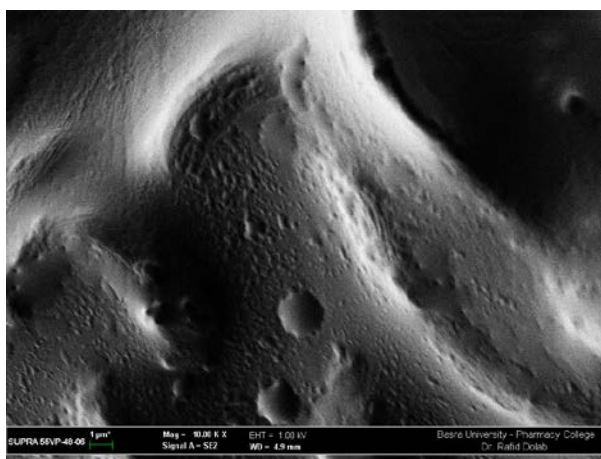Figure (14) showing histological section of parotid gland, the surface of tissue. 10µm.

Figure (15) showing histological section of parotid gland, the surface are contain invagination aleveole.1µm.

Ultrastructure of submandibular gland:
In submandibular gland, coarser bundles of collagen fibers traversing the interracial spaces and linking neighboring acini were furthermore observed in figure (16). At high magnification, the extremal surfaces of the acinar secretory cells contained small-diameter connective tissue fibrils that were intimately associated and sometimes embedded within the basement membrane of the cells, which clarify in figure (17).

The serous cells are observed clearly that arranged around lumen forming structure as tubules, network of inter-lobar collagen fiber connective tissue provide confirm these structure. These fibers tightly connecting serous cell with each other, for arranged in tubule structure. The mucous acini that arranged in alveoli structure. The MECs that showing clearly around serous cells and mucous cells that clarify in figure (16), and high resolution of the serous tubules that state in figure (17, 18, 19).

In figure (17) represent the mucous acini next the serous tubules and the intercalated duct that clear consist of simple cuboidal cells in figure around by connective tissue fiber and MECs.

In figure (19) that elucidate the high magnification of SEM observed the serous tubules structure is clearly found in center of image, show the junction between serous tubules and intercalated duct. That shown cells in the serous tubules are pyramidal shape and larger than one layer of cuboidal cells in the intercalated duct. In that, the serous cells were arranged one each other that formed tubule structure, its rounded by MECs (white arrow). the MEC have four primary cytoplasmic processing that shown these primary cytoplasmic processing are shorter and branching to final cytoplasmic processing (secondary, tertiary) that arranged around serous cells may be for initiation squeezing the cell. Mucous acini between them, and network of intra-lobar collagen fiber connective tissue connected each other. In same figure observed MEC catching the serous cell. The MEC (in white arrow) have five primary cytoplasmic processing shown thicker processing and branching to form many final cytoplasmic processing that reinforcing underlying the mucous cell.

In figure (19) expound the mucous cells arranged in acini and observed MEC (in white arrow) have six primary cytoplasmic processing around mucous acini . The right above the image shown the serous tubules, but down in same side shown the connective tissue fibers. The MEC (in white straight) it's have five primary cytoplasmic processing shown longer and thinner processing and little branching to form many final cytoplasmic processing. Under (star shape) the MEC have five primary cytoplasmic processing 0.5 µm that like the result that clarify in the figure (19) that seen the final cytoplasmic processing less compear with the MEC have six primary cytoplasmic processing.

In the figure (20) shown the mucous acini were rounded by MECs that send primary and secondary cytoplasmic processes, some of final cytoplasmic processes extended to adjacent cells in the same acini. In figure (22) clarify the MEC on surface of mucous cell as well as observed three aggregation of particles in above right of the image may be this protein integrin of the desmosome and shown the fiber of basal lamina this fibers may be collagen fiber type III.
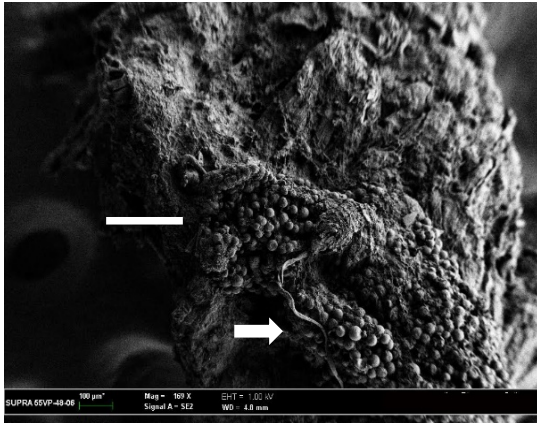
Figure (16): showing histological section of submandibular gland, serous tubules and three-dimensional supporting inter-lobar connective-tissue network is observed with bundles of collagen fibers spanning (white star) and observed serous tubules (white seriated) and mucous acini (white arrow).100µm.
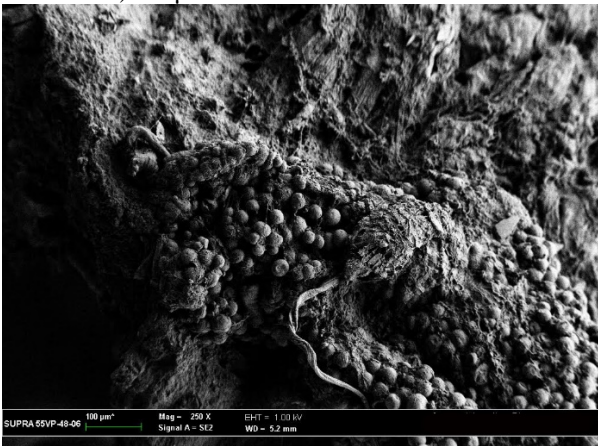
Figure (17): Showing histological section of submandibular gland in SEM, serous tubules and three-dimensional supporting inter-lobar connective-tissue network is observed with bundles of collagen fibers spanning (white star) and observed serous tubules (white seriated) and mucous acini (white arrow).100µm.

Figure (18): showing histological section of submandibular gland in SEM, mucous acini (white arrow) next serous tubules (white seriated) attached to the intercalated duct (white star) and. The MEC have four primary cytoplasmic processing100µm.

Figure (19): showing histological section of submandibular gland in SEM, show the junction between serous tubules and intercalated duct. That shown cells in the serous tubules are pyramidal shape and larger than one layer of cuboidal cells in the intercalated duct. 20µm.

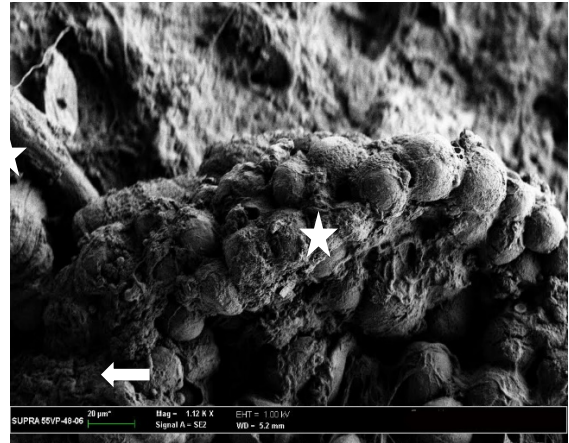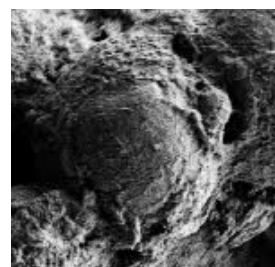

Figure (20): showing histological section of submandibular gland, MECs have four primary cytoplasmic processes. 10µm.
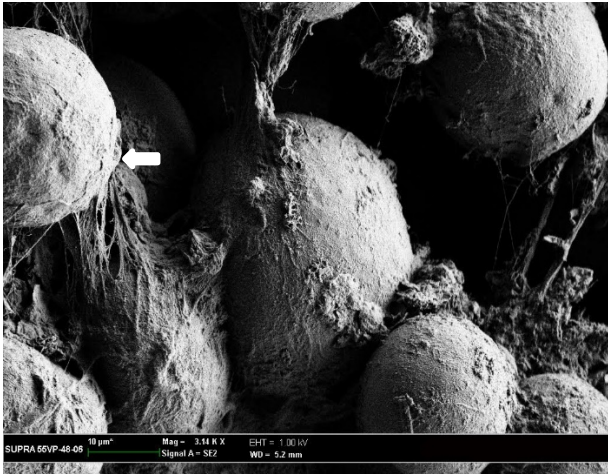
Figure (21): showing histological section of submandibular gland, A three-dimensional ob..... .ed serous tubules with bundles of collagen fibrils spanning10μm
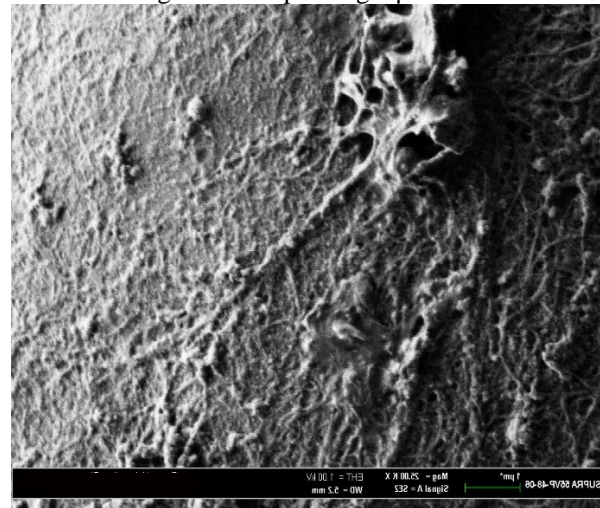

Figure (22): showing histological section of submandibular gland, the surface of mucous cell and MEC on their surface, the fibers of basal lamina are showed, 1μm.

Ultrastructure of sublingual gland:

In the figure (24, 25) expound the serous cell in above the image smaller in size than he mucous cell underling also the mucous acini are elongated and catching by MEC are extending their primary cytoplasmic processing on mucous cell and plug in terminal ending that sending many final cytoplasmic processing, also each branch are forming plug.

Under SEM the image of submandibular gland that observed the primary cytoplasmic processing are formed plug in terminal ending and have many final cytoplasmic processing. Also showing the collagen fiber type three in basal lamina of mucous cell. These fibers are reticular fiber forming network structure. Which expound in figure (26). Furthermore shown terminal end fibers that located between the near the end the primary cytoplasmic processing of MEC.
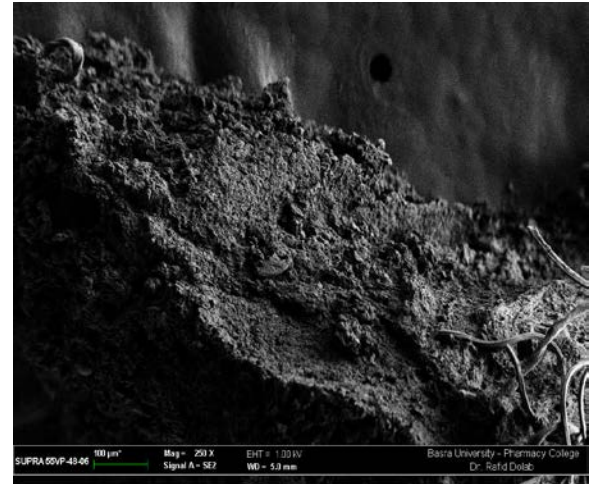
Figure (23): showing histological section of sublingual gland, the surface of tissue, three-dimensional of collagen fibrils spanning100μm.

Fig (24): showing histological section of sublingual gland, A three-dimensional section with showing mucous, serous cell and myoepithelial spanning10μmFigure (25) showing histological section of sublingual gland, A three-dimensional section with showing mucous, serous cell and myoepithelial spanning there primary cytoplasmic processing 10μm.
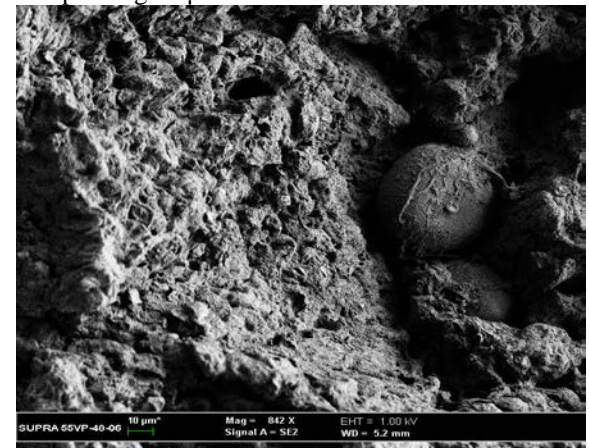

Figure (4.25) showing histological section of sublingual gland, A three-dimensional section with showing free end of primary cytoplasmic processing of the MEC are forming plug structure panning the final cytoplasmic processing. SEM. 2μm
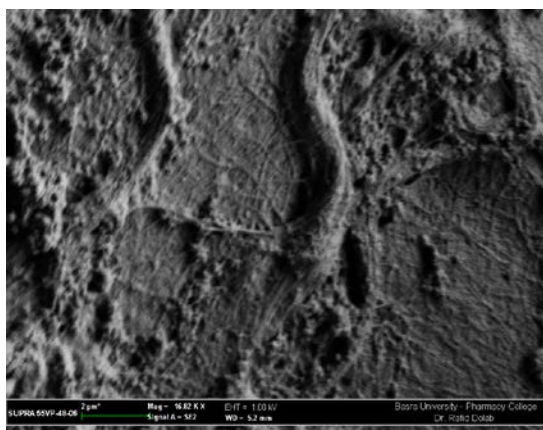
Figure (26) showing histological section of sublingual gland.

DISCUSSION:

The estimation the electrolytes Iodide, Sodium, potassium calicum, phosphate, sulfate and carbonate in the salivary gland tissue:

In current study measured the electrolyte in the tissue of major salivary gland before measure it the tissue treated by osmium until the tissue black color for they excretion all saliva from the ductal system for measure the electrolyte only in tissue.

In present study, the table (1) show the increase concentration of the inorganic iodine electrolyte in the submandibular gland tissue comparative with the parotid and sublingual gland respectively.

Paulev and Zubieta-Calleja (2017), performed the submandibular gland that explain the inorganic iodine regulated secretory the EGF. As well as when secretory of EGF from mucous acini that drain in to ducts, in striated duct the amount EGF release in to the blood stream that effect on thyroid to decrease utilized the iodine (Dagogo-Jack, 1994).

Previously study by researchers Suciu1*et al.* (2017), the NIS is a 643 amino corrosive protein and contains 643 transmembrane areas. The sub-atomic portrayal of sodium iodide symporter (NIS). Despite the fact that there are similitudes both the salivary and thyroid iodine concentrating instrument.

The physiological researchers Portulano, Paroder and Carrasco (2014), their study reported The physiological part of iodide discharge in the saliva involves banter. Given to its cancer prevention agent properties, iodide may go about as an antimicrobial operator in saliva. A bactericida bacteriostatic impact of iodide is predictable with the nearness of a H2O2/peroxidase role in the salivary glands. (Bergström, 2004). In the salivary gland, NIS is profoundly communicated in the basolateral films of the larger part of striated conduits. (La Perle *et al.,* 2013).

The researcher Haiyoung Son. (2017), reported of the iodine are play important role of the regulation of salivary gland when deficiency of iodine with cancer of thyroid gland of patient also causes salivary gland dysfunction. However, when supplement iodine daily that reduce salivary glands damage. (Liu *et al.,* 2010; Jentzen *et al.*,

2014; Ko, *et al*., 2015; Klein Hesselink *et al.,* 2016; Badam *et al*., 2016; Maruoka, 2017).

Where is the tight junctional conductance and Na^+ or K^+. We find we can attain the final saliva (Nakamoto *et al*., 2008).

The researcher Perle and vesticator (2013), reported that studies on human NIS found in striated duct cells in submandibular salivary glands was more prominent than in parotid salivary gland, recommending a higher clearance rate of saliva discharge in submandibular salivary glands. NIS articulation in striated ducts. Dietary insufficiency or overabundance of iodine has a critical part in buccal mucosa as well as salivary glands physiology. Salivary glands got from crude iodine concentrating oral cells, which amid embryonic development, move and work in discharge of saliva with iodine. "Gastro-salivary clearance" and discharges of iodides are a significant piece of "gastro-intestinal cycle of iodides", that institutes around 23 percentage of iodine pond in the human body.

Venturi and Venturi, (2009), performed the organs such as the salivary glands, stomach and thyroid offer uptake of iodine by sodium iodide symporter (in NIS that inter iodine versus sodium) and peroxidase action (transference electrons from I to the oxygen of H2O2 thus shields the cells named peroxidation).

Previously study by Vayre *et al*. (1999), performed the sodium/iodide symporter (NIS) is a complex protein located in the basolateral position of the cell membrane of the majority of striated ducts in salivary glands. However, feebly communicated in few intercalated and excretory duct cells. Also, found in follicular cells in the thyroid glands. The NIS allow one iodide inside the cell exposure Na outside. (Jhiang *et al*., 1998).

We suggest the iodide increase in the submandibular gland tissue than the other salivary glands, because contain high number of straited ducts, which contain the NIS in basolateral columnar cells that allow inter high number of iodide.

In current, study that experimental on domestic rabbit of salivary gland when measure the electrolyte that reported increase concentration of the Na+ in the submandibular gland followed it the sublingual and parotid glands tissue.

Previously study by Zhang *et al*. (2017), performed an intact salivary gland secretes their secretion into two phases. To begin with, acinar cells create primary saliva, their composition similar to a plasma, isotonic liquid which highly sodium and chloride concentration. The other phase, which the ducts replace sodium and chloride by potassium and compound HCO3−, creating a hypotonic last saliva nerveless misfortune (decrease) in volume. (Patterson *et al*., 2012).

Gorr and Abdolhosseini (2011), reported in their study the inside saliva spit, K+ fixations increment while Na+ focuses diminish within the sight of antidiuretic hormone (ADH) or aldosterone. Not at all like other stomach related organs, be that as it may, these two hormones don't influence salivary glands discharge rate. The increase concentration of sodium in the submandibular gland may be beyond to increase effected antidiuretic hormone (ADH) or aldosterone on the cellmemrane of the glandular cells to

reapsorption of Na+ ion and secretion of K+ ion in saliva. Thithe increase concentration Na+ in submandibular gland tissue than the parotid gland tissue. The increase concentration Na+ in saliva may be that indicator increase the flow rates, while Na+ concentration in parotid gland is low may be caused by secreted sodium in saliva. May be theis increase sodium in submandibular gland tissue when mapping analysis the reason beyond the Sodium chloride absorption by striated ductal cells are more compared with the sublingual and parotid gland.

In current result they increase Ca2+ concentration in the submandibular gland tissue comparative with the sublingual and parotid gland respectively. When increase the activity of the acini. The physiological researchers Patterson et al. (2012), when study the "electron neutral anion exchanger" in the basement Lumina of the salivary gland cells, recommends the electronic interchange of the anion has fewer impact in the submandibular salivon. Demonstrated that the inwardly rectifying potassium current and Bk channels (also named maxi-K) directs in parotid salivary organ acinar cells are hyperpolarization of cells from by the electrogenic Na(+),K(+)- ATPase (Ko et al., 2004; Romanenko et al., 2007). Romanenko, et al. (2010), performed TMEM16A, which we additionally call anoctamin 1 (ANO1) new group of ionic channels is a real Ca2+-actuated chloride channel that is initiated by intracellular Ca2+ and Ca2+-preparing boosts. With eight putative transmembrane domains and no evident closeness to beforehand portrayed channels. The biophysical properties and the pharmacological profile of ANO1 are in full concurrence with local Ca2+-actuated chloride streams (Y. D. et al. 2008).

In current, result the increase of concentration the potassium electrolyte in the submandibular gland tissue comparative with the parotid and sublingual gland respectively. The researcher Reynolds and Pull (1983) reported the high concentration of the sodium and chloride but the potassium reported lower concentration in saliva of submandibular of rabbit. The concentration of electrolyte in ductal system in gland that depending the maturation of the striated ducts. Previously study by Romanenko et al., (2007), performed The sodium/iodide symporter (NIS), Na(+),K(+)-pump, that found greater in the submandibular gland comparative with the parotid and sublingual glands. . (Vayre et al., 1999).

According these research that supported our result increase concentration the Na (+), K (+) in the submandibular gland when measure it's in EDS. Mangos et al., (1973), reported as the stream rate increments ("along the x-axis"), unmistakably the Na+ and Cl− ingestion diminishes, coming about more Na+ and Cl− in conclusive spit. Likewise, K+ emission diminishes, bringing about less K+ in conclusive spit. The movement of the Liquid and electrolyte determined by transmembrane Cl- gate channels. These channels are concerned on the supra-membrane of acinar cells starts the fluid discharge mode. However, the actuation of Cl- channels in the cells ductal system are contributed in both portion the apical and the basolateral portion of the cells for Sodium chloride re-ingestion.

Previous study by physiological research Petersen (2017), performed Upwards of several classes of chloride channels with particular gating systems can be distinguished in salivary gland. Such as, Cl-channels is actuated by intracellular calcium, An expansion in the intracellular free Ca2+ fixation is the predominant system activating liquid emission from acinar cells. Other class, Cl-channels is gated by cAMP, for effective NaCl re-assimilation in numerous ductal cells. (Crampin, 2012; Almassy and Yule, 2013). Maclaren, et al. (2012), performed the chloride gated channels, rapidly prompted changes in membrane active potential as well as, cell volume motivate distinctive chloride gated channels that expected play important role for regulating the liquid and electrolyte development. (Melvin, 1999; Nakamoto et al., 2008; Palk et al., 2010). Previous study by physiological researchers Shcheynikov et al. (2008), performed Transcellular Cl− and HCO3− transport is a essential capacity of secretory epithelia and exit over the luminal membrane is interceded by members of the SLC26 transporters related to with cystic fibrosis transmembrane conductance regulator (CFTR) channel. Previously study by Almássy J et al. in 2018, performed the osmotic gradient is made by the apical Cl− efflux and the ensuing para-cellular Na+ transport. In this fashion, the Na+-K+ pump is found solely in the basolateral film and has basic job in salivary discharge, however, the driving force for Cl− transport by means of basolateral Na+− K+− 2Cl− cotransport is created by the Na+-K+ pump. What's more, the constant electrochemical gradient for Cl− flow through acinar cell stimulation is kept up by the basolateral K+ efflux (Palk et al., 2010).

In current, result the increase of concentration the Carbone and oxygen in the parotid gland tissue comparative with the submandibular and sublingual gland respectively.

Park et al. (2010), performed in their study the secreted of saliva from secretory end-piece always, high concentration of Na+. After that replaced the Na+ by K+ in striated ducts. However, the finally saliva are high concentration of K+ and low concentration of Na+. but when increase the flow rate of saliva from salivon, they increase, Na+ and Cl− in saliva, while decrease concentration of K+, but (HCO3−) remain constants. As it were, Na+ and Cl− are for the most part emitted and afterward gradually, reabsorbed along the course of the salivary framework, from acinus to ducts (Li et al., 2006; Holsinger and Bui, 2007).

May be related the bicarbonate ion increase in the parotid glandthe high flow rate not causes increase the secretion carbonate in saliva.

In current, result the increase of concentration the sulfate in the submandibular gland tissue comparative with the sublingual and parotid gland respectively. Bancroft, Suvarna and Layton (2013). That may be related the mucin of acinar cell are contain slio-mucin (sulfate mucin) the positive to alcin blue indicted of the acidic mucin and sulfate mucin) the researchers Al-Saffar and Simawy, (2014) for strongly positive with alcin blue stain of submandibular gland.

Ultrastructure of the three major salivary gland by electron microscope:
Scanning electron microscope (SEM).
Ultrastructure of MECs

The MECs under SEM detail's the MECs have few primary cytoplasmic processes that longer and thinner primary cytoplasmic processes and in free end are few branching final cytoplasmic processes, And the some primary cytoplasmic processes are extending in to other cell in same acini or along serous tubules and intercalated duct, that show Figure (18). Often these MECs have three or four primary cytoplasmic processes that found around serous tubules and intercalated duct. Whereas the MECs have five, six primary cytoplasmic processes are shorter, and thicker primary cytoplasmic processes the free end are forming plug and then forming final cytoplasmic processes. The final cytoplasmic processes are large in numbers and formed around cells always, mucous cells.

Previously study Nagashima and Ono (1985), when study of MEC in human submandibular glands by Transmission electron microscopy performed, two kind of MECs can be distinguished. (One) The dark MEC kind, was stellate-like shape and showed an articulated electron density shown many numbers of myofilaments and represented around 76% of MEC. Showed ATP activity. (Second) The light MEC kind, was large size and ellipsoid shape with a little number of the short thickness cytoplasmic processes and observed positive ATPase activity and represented just 17% from the total MEC count, transitional forms between these two kinds were likewise watched, moreover the light MEC kind may develop into the dark MEC type.

The recent study by Gnepp (2001) performed when examination the salivary gland under SEM furthermore exposed that MEC processes subdivide into several secondary and tertiary divisions, there probably to thirty terminal processes extending from each MEC, some of MEC primary cytoplasmic processes expound thicker MEC processes than others with more viscous secretions.

Ultrastructure of parotid gland:

Parenchymal and stromal component parotid gland were scanning electron microscopy (SEM). Fixative 2.5ml glutaraldehyde and 2.5ml formalin 10

better differentiate connective tissue and cellular components. What's more, the inside three-dimensional morphology of the secretory acinar cells and duct cells was uncovered by maceration with a diluted the osmium tetroxide solution for specifically evacuate. Some of the cytoplasmic components. SEM examination parotid glands revealed a fine filamentous network immediately surrounding each acinus. The bundle of collagen fibers are bind with adjacentcell.

The researchers Watanabel and fustigator (1996) performed when scanning electron microscope examination of salivary gland shown three-dimensional structure of the connective-tissue fibers. Each lobules are rounded by a dense regular collagen fibers. Probably the connective tissue are inter-lobar connective tissue between the lobules.

Additionally, coarser bundles of collagen fibers traversing the intra-lobular spaces and linking neighboring acini. At high striated ducts embedded in the connective-tissue septa

can be observed in figure (8). Each lobule was surrounded by a dense network of collagen fiber in inter-lober connective tissue, that appeared to be continuous with the interracial connective-tissue stroma. in figure (5, 6, 7) the acini seem embedding in collagen fiber in inter-lober connective tissue.

In the figure (12) shown clearly the striated duct. The surface of the striated duct are longitudinal threat like structure. The researchers Park, Evans and Watson (2001) probably, the basal region of the columnar cells are many folded in these folded found mitochondria arranged vertically on basement membrane. May be related the arranged fibers of connective tissue longitudinally around striated.

In the figure (13) shown serous cells are pyramidal in shape and very small. In books cats of oral histology for Nanci A. in 2013, probably the serous cell are pyramidal in shape with basement membrane in the base and small size. May be suggested the image under SEM are serous cell.

In the figure (14, 15) shown the outer surface is not smooth contain abundant alveolar invaginations in areas that observed in SEM. The researcher Nanci A. mention of their book in 2013, the external surface of the MECs are not smoothly that containing many invagination area for attached with the terminal nerve fiber of the parasympathetic nerve tidal from parasympathetic nerve ganglion, The cilia of the MEC are projected into these invaginations may act as chemoreceptors. May be these alveolar invaginations in areas beyond to the place attached with of the parasympathetic nerve.

Ultrastructure of submandibular gland:

In figure (16) of the submandibular gland, coarser bundles of collagen fibers traversing the interracial spaces and linking neighboring acini. The researcher Cui D *et al.* (2011) performed in their book Atlas of Histology with Functional and Clinical Correlations the connective tissue among the lobules and surround them. Probably network of inter-lobar collagen fiber connective tissue provide confirm these structure. In figure (17, 18) shown the mucous acini next the serous tubules and the intercalated duct that clear consist of simple cuboidal cells in figure aroud by connective tissue fiber and MECs.the researchers Toyoshima K. and Tandler B.in 1986 performed the serous cell in submandibular gland of the rabbits are arranged as serous tubules between secretary end pieces the mucous acini and intercalated duct. May be these image of SEM show the junction between serous tubules and intercalated duct. That shown cells in the serous tubules are pyramidal shape and larger than one layer of cuboidal cells in the intercalated duct. in that the serous cells are arranged one each other that formed tubule structure,

In figure (19) the MEC have five primary cytoplasmic processing that shown these primary cytoplasmic processing are shorter and branching to high number of final cytoplasmic processing that reinforcing underlying serous cells for initiation squeezing the cell Mucous acini between them. The MECs are hybed that have mesenchymal charecters that contain contractile myofilament, the actin myofilament that arranged flask-like shape underlying basal lamella of MEC along primary and

final cytoplasmic processing and binding with vimentin in this the tandler expound the action of ATPase when found several enzymes, these enzymes indicator for contractile function of MECs, such as Emmelin and garrent, furthermore clarify single electrical for parasympathetic nerve. The terminal end of the parasympathetic nerve ley between MEC and acini cell. (Carpenter *et al.*, 2008; Zhang *et al.*, 2018).

In figure (19) shown the mucous cells arranged in acini and observed MEC have six primary cytoplasmic processing around mucous acini and the MEC it's have four primary cytoplasmic processing shown longer and thinner processing and few branching to form many final cytoplasmic processing. Under the MEC have five primary cytoplasmic processing 0.5 µm that like the result in the figure (12) that seen the final cytoplasmic processing less compear with the MEC have six primary cytoplasmic processing. The researcher Brocco and Tamarin, (1979), performed analysis of MECs by scanning electron microscopy the MECs have many cytoplasmic processes and these processing are branched many times. Some of these processing have more branched.

in figure (22) clarify the MEC on surface of mucous cell as well as observed three aggregation of particles in above right of the image may be this protein integrin of the desmosome.

Desmosomes were a reliable component of the surface of the acinar cell as were singular cilia. The last structures were generally situated in the intercellular space among myoepithelium and secretory cell, however at times a cilium expanded profoundly into an invagination of the secretory cell (Tandler, 1997; Junqueria and Carneiro, 2011).

Ultrastructure of sublingual gland:
In the figure (25) showing the serous cell in above the image smaller in size than he mucous cell underling also the mucous acini are elongated and catching by MEC are extending their primary cytoplasmic processing on mucous cell and plug in terminal ending that sending many final cytoplasmic processing, also each branch are forming plug. The researchers Cui *et al.* (2011) mention in the book Atlas of Histology with Functional and Clinical Correlations the size of the serous cell are very smaller than the mucous acini. Serous cells are arranged into many small acini or serous cells are caped around mucous acini as (serous Demilune), however, the mucous cells are arranged as acini or tubular structures.

Under SEM the three dimension image of sublingual gland that observed the primary cytoplasmic processing are formed plug in terminal ending and have many final cytoplasmic processing. Also showing the collagen fiber type three in basal lamina of mucous cell. These fibers are reticular fiber forming network structure. Shown in figure (26). Furthermore shown terminal end fibers that located between the near the end the primary cytoplasmic processing of MEC.

May be ancient study by several researchers that mention in addition the contractile role of MECs also have responsible for conduction neural stimulation and participate in signaling the secretory cells that the terminal end of parasympathetic nerve fiber lies between MECs and parenchymal cell of the acini (Ogawa, 2003; Kumar, 2008; Ianez *et al.*, 2010; Chitturi *et al.*, 2015).

REFERENCE

1. Almassy J. and Yule D I. (2013). Investigating ion channel distribution using a combination of spatially limited photolysis, Ca(2+) imaging, and patch clamp recording. Cold Spring Harb Protoc (1).
2. Al-Saffar F. J. and Simawy M. S. H. (2014). Histomorphological and histochemical study of the major salivary glands of adult local rabbits ISSN 2320-5407 International Journal of Advanced Research, Volume 2, Issue 11, 378-402
3. Alvarez-Castaneda S.T.; Alvarez, T. and Gonzalez-Ruiz, N. (2017), Keys for Identifying Mexican Mammals,. Johns Hopkins University Press, Baltimore, Maryland pp. 229- 240.
4. Ambudkar, IS. (2014). Ca (2)(+) signaling and regulation of fluid secretion in salivary gland acinar cells. Cell Calcium, 55(6), 297-305.
5. Badam RK., Suram J., Babu DB., Waghray S., Marshal R., Bontha SC. (2016). Assessment of Salivary Gland Function Using SalivaryScintigraphy in Pre and Post Radioactive Iodine Therapy in Diagnosed Thyroid Carcinoma Patients. J Clin Diagn Res. ;10(1):ZC60–62.
6. Bancroft JD, Suvarna SK. and C Layton C (2013). Bancroft's theory and practice of histological techniques. Elsevier Limited. All rights reserved. Seventh edition. (12): pp 220-228.
7. Bergström J. (2004). Tobacco Smoking And Chronic Destructive Periodontal Disease. Odontology. 92(1):1-8.
8. Brini, M., and Carafoli, E. (2011). The plasma membrane ca (2)+ ATPase and the plasma membrane sodium calcium exchanger cooperate in the regulation of cell calcium. Cold Spring Harbor Perspectives in Biology, 3(2),10.
9. Brocco, S. L. and Tamarin, A. (1979). The topography of rat submandibular gland parenchyma as observed with SEM. *Anat. Rec.* 194; 445–460.
10. Buseth ME. and Saunders R. (2014) Rabbit Behaviour, Health and, Printed and bounded by Gutenberg Press Ltd., Tarxien, Malta. Care, CABI ed. pp. 1-13.
11. Carpenter GH, Khosravani N., Ekström J., Osailan SM., Paterson KP. and Proctor GB. (2008). Altered plasticity of the parasympathetic innervation in the recovering rat submandibular gland following extensive atrophy. Exp Physiol. 2009 Feb;94 (2): 213-219.
12. Cruchley AT. and Bergmeier LA. (2018). Structure and Functions of the Oral Mucosa. Oral Mucosa in Health and Disease pp 1-18.
13. Cui D., Naftel J P., Lynch J C., Yang G., Daley W P., Haines D E. and Fratkin J D. (2011). Digestive Glands and Associated Organs of the Atlas of Histology with Functional and ClinicalCorrelations. Lippincott Williams & Wilkins, a Wolters Kluwer business. Toyoshima K. and Tandler B. (1986). Ultrastructure of the Submandibular Gland in the Rabbit Department of Oral Biology, School of Dentistry (K. 71, B. T), Case Western Reserve University, Cleveland, Ohio 44106. The American Journal of Anatomy 176:469-481.
14. Dagogo-Jack S (1994). Dietary iodine affects epidermal growth factor levels in mouse thyroid and submaxillary glands. Endocr Res. Aug; 20(3):247-57.
15. Gnepp DR. (2001). Diagnostic Surgical Pathology of the Head and Neck. 2nd edition. Philadelphia: W. B. Saunders Co; ch; 6: 789-823.
16. Gorr S.G. Venkatesh and Darling D.S. (2005). Parotid Secretory Granules: Crossroads of Secretory Pathways and Protein Storage. Department of Periodontics, Endodontics and Dental Hygiene and Center for Oral Health and Systemic Disease, University of Louisville School of Dentistry, Louisville, KY 40292, USA; J Dent Res. Jun;84(6):500-9.
17. Holsinger F. C. and Bui T.D. (2007). Anatomy, Function, and Evaluation of the Salivary Glands. of salivary gland disorder. Springer Berlin. Heidelberg: pp 1-16.
18. Jentzen W., Richter M. and Nagarajah J. (2014). Chewing-gum stimulation did not reduce the absorbed dose to salivary glands during radioiodine treatment of thyroid cancer as inferred from pre-therapy (124)IPET/CT imaging. EJNMMI Phys; 1: 100-102.
19. Jhiang SM., Cho JY., Ryu KY., DeYoung BR., Smanik PA., McGaughy VR., Fischer AH. and Mazzaferri EL. (1998). An immunohistochemical study of Na$^+$/I$^-$ symporter in human thyroid tissues and salivary gland tissues. Endocrinology.;139:4416–4419.
20. Junqueria L. and Carneiro J. (2011) Basic Histology: Text & Atlas., Tenth edn. McGarrow-Hill, New York.; (16): 323-331.
21. Junqueria L. and Carneiro J. (2011) Basic Histology: Text & Atlas., Tenth edn. McGarrow-Hill, New York.; (16): 323-331.

22. Klein Hesselink EN., Brouwers AH. and de Jong JR (2016) Effects of radioiodine treatment on salivary gland function in patients with differentiated thyroid carcinoma: a prospective study. *J Nucl Med*; 57: 1685-91.

23. La Perle K M., Kim DC., Hall NC., Bobbey A., Shen DH., Nagy RS., Wakely PEJ., Lehman A., Jarjoura D., and Jhiang SM. (2013). Modulation of Sodium/Iodide Symporter Expression in the Salivary Gland. Thyroid. 2013 Aug; 23(8): 1029–1036.

24. Lamy E., Capela-Silva F. and Tvarijonaviciute A. (2018). Research on Saliva Secretion and Composition *Editorial* Hindawi BioMed Research International Volume, Article ID 7406312- 2.

25. Li J., Koo N Y., Cho I H., Kwon T H., Choi S Y., Lee S J., Oh SB., Kim JS. and Park K. (2006). Expression of the Na^+-HCO_3^- cotransporter and its role in pH_i regulation in guinea.

26. Liu B., Kuang A., Huang R. et al. (2010). Infuence of vitamin C on salivary absor-131 bed dose of I in thyroid cancer patients: a prospective, randomized,single-blind, controlled trial. *J Nucl Med*; 51: 618-23. Ko KY., Kao CH. and Lin CL. (2015). (131)I treatment for thyroid cancer and the risk of developing salivary and lacrimal gland dysfunction and a second primary malignancy: a nationwide population-based cohort study. Eur J Nucl Med Mol Imaging; 42: 1172-1178.

27. Maclaren O, Sneyd J. and Crampin E. (2012). Efficiency of primary saliva secretion: an analysis of parameter dependence in dynamic single-cell and acinus models, with application to aquaporin knockout studies. J Membr Biol 245: 29–50.

28. Mangos JA, McSherry NR, Nousia-Arvanitakis S. and Irwin K. (1973). Secretion and transductal fluxes of ions in exocrine glands of the mouse. Am J Physiol 225: 18–24.

29. Maruoka Y., Baba S., Isoda T., Kitamura Y., Koichiro Abe, Masayuki Sasaki, and Honda H. (2017). A Functional Scoring System Based on Salivary Gland Scintigraphy for Evaluating Salivary Gland Dysfunction Secondary to ^{131}I therapy in Patients with Differentiated Thyroid Carcinoma. J Clin Diagn Res. Aug; 11(8): TC23–TC28.

30. Melvin JE. (1999). Chloride channels and salivary gland function. Crit Rev Oral Biol Med.;10(2):199-209.

31. Nagashima Y. and Ono K. (1985). Myoepithelial cell ultrastructure in the submandibular gland of man. Anat Embryol (Berl);171:259-65.

32. Nakamoto T., Romanenko VG., Takahashi A., Begenisich T. and Melvin JE. (2008). Apical maxi-K ($K_{Ca}1.1$) channels mediate K^+ secretion by the mouse submandibular exocrine gland. Am J Physiol Cell Physiol 294: C810–C819.

33. Nanci A. (2012). Ten Cate's Oral Histology: Development, Structure, and Function. 8 [th] ed. Pheladelphia: Elsevier Mosby ;(1); 290-317.

34. Nanci A. (2012). Ten Cate's Oral Histology: Development, Structure, and Function. 8 [th] ed. Pheladelphia: Elsevier Mosby ;(1); 290-317.

35. Ohtomo, K., Shatos, MA., Vrouvlianis, J., Li D., Hodges, RR. and Dartt, D. A. (2011). Increase of intracellular Ca2+ by purinergic receptors in cultured rat lacrimal gland myoepithelial cells. Investigative Ophthalmology & Visual Science, *52*(13), 9503-9515.

36. Palk L, Sneyd J, Shuttleworth TJ, Yule DI, Crampin EJ. (2010). A dynamic model of saliva secretion. J Theor Biol 266: 625–640.

37. Park HW., Nam JH., Kim JY., Namkung W., Yoon JS., Lee JS., Kim KS., Venglovecz V., Gray MA., Kim KH. and Lee MG. (2010). Dynamic regulation of CFTR bicarbonate permeability by $[Cl^-]_i$ and its role in pancreatic bicarbonate secretion. Gastroenterology 139: 620–631.

38. Park K., Evans RL. and Watson GE. (2001). Defective fluid secretion and NaCL absorption in the parotid glands of Na+/H= exchanger-deficient mice. JBiol. Chem.; 76:27042-50.

39. Patterson K., Catalán M A., Melvin J E., Yule D I., Crampin E J., and Sneyd J (2012). A quantitative analysis of electrolyte exchange in the salivary duct Am J Physiol Gastrointest Liver Physiol. Nov 15; 303(10): G1153–G1163.

40. Paula FD., Harumi T., Hsieh TN., Souza MM, Nico MM And Lourenco SV. (2017) Overview Of Human Salivary Glands: Highlights Of Morphology And Developing Processes. THE Anatomical Record 300:1180–1188.

41. Paula FD., Harumi T., Hsieh TN., Souza MM, Nico MM And Lourenco SV. (2017) Overview Of Human Salivary Glands: Highlights Of Morphology And Developing Processes. THE Anatomical Record 300:1180–1188.

42. Paulev PE. and Zubieta-Calleja G. (2017) Thyroid hormones and disorders. In: Textbook in Medical Physiology and Pathophysiology Essentials and Clinical Problems, 2nd edn.

43. Petersen OH. (2017). The effects of Ca2+ buffers on cytosolic Ca2+ signalling, The Journal of Physiology, 595, 10, (3107-3108).

44. pig salivary glands. Am J Physiol Gastrointest Liver Physiol 291:1031–1040.

45. Portulano C., Belenitsky – Paroder and Carrasco N. (2014). Endocrine Reviews. 35(1):106-149.

46. Proctor G. B. (2016). The physiology of salivary secretion. Periodontology. John Wiley & Sons A/S. Published by John Wiley & Sons Ltd. Periodontology 2000, Vol. 70(1): 11-25.

47. Proctor GB. and Carpenter GH. (2014) Salivary Secretion: Mechanism and Neural Regulation. Anatomy and Physiology Ligtenberg AJM, Veerman ECI (eds):. Monogr Oral Sci. Basel, Karger, vol 24, pp 14-29.

48. Reynolds JM. and Pull SL. (1983). The concentration of sodium, potassium and chloride in rabbit submandibular saliva during postnatal development. Archives of oral biology .Volume 28, Issue 9, page 879-883.

49. Romanenko V, Thompson J. and Begenisich T (2010). Ca^{2+}-activated K channels in parotid acinar cells: the functional basis for the hyperpolarized activation of BK channels. Channels (Austin) 4:278–288 .

50. Romanenko VG., Catalan MA., Brown DA., Putzier I., Hartzell HC., Marmorstein AD., Gonzalez-Begne M, Rock JR, Harfe BD, Melvin JE. (2010). Tmem16A encodes the Ca2+-activated Cl_channel in mouse submandibular salivary gland acinar cells. J Biol Chem: 285: 12990–13001.

51. Romanenko VG., Nakamoto T., Srivastava A., Begenisich T., Melvin JE. (2007). Regulation of membrane potential and fluid secretion by Ca^{2+}-activated K^+ channels in mouse submandibular glands. J Physiol 581: 801–817.

52. Roussa, E. (2011). Channels and Transporters In Salivary Glands. Cell Tissue Res (Freiburg, Germany), 343, 263–287.

53. Segawa A., Loffredo F., Puxeddu R., Yamashina ST., esta Riva F. and Riva A. (2000). Cell biology of human salivary secretion. Eur J Morphol: (38): 237–241.

54. Shcheynikov N., Yang D. , Wang Y., Zeng W. , Karniski LP., Insuk So., Wall SM. and Muallem S. (2008). The Slc26a4 transporter functions as an electroneutral $Cl^-/I^-/HCO_3^-$ exchanger: role of Slc26a4 and Slc26a6 in I^- and HCO_3^- secretion and in regulation of CFTR in the parotid duct. The Journal of Physiology. Ph.S: 79.

55. Son H., Lee SM., Yoon RG., Lee H., Md IL., Kim S., Chung WY. and Lee JW. (2017). Effect of selenium supplementation for protection of salivary glands from iodine-131 radiation damage in patients with differentiated thyroid cancer. Hell J Nucl Med; 20(1): 62-70.

56. Suciu I., Ionescu E., Suciu I., Chirila1 M., Gheorghe I., Popa M., Dumitriu1 A., Horia Ursu (2017). First Report In Romania Regarding Salivary Iodine Level And Its Correlation With Carious Lesions, Chronic Marginal Periodontitis And Periapical Pathology. Romanian Biotechnological Letters. University of Bucharest. Vol. 21, No. x.

57. Tandler B, Nagato T, Phillips CJ. 1997b. Ultrastructure of the unusual accessory submandibular gland in the fringe-lipped bat, *Trachops cirrhosus*. Anat Rec 248:164–175.

58. Tandler B., Gresik E. W., Nagato T., and Phillips C. J. (2001) Secretion by striated ducts of mammalian major salivary glands: review from an ultrastructural, functional, and evolutionary perspective. Anat. Rec.; 264:121–145.

59. Vayre L. Sabourin JC. Caillou B. and Ducreux M. (1999). Schlumberger M. Bidart JM. Immunohistochemical analysis of Na^+/I^- symporter distribution in human extra-thyroidal tissues. Eur J Endocrinol.;141: 382–386.

60. Venturi S. and Venturi M. (2009). "Iodine in evolution of salivary glands and in oral health". Nutrition and Health. 20 (2): 119–34.

61. Watanabe H. Seguchi T. Okada T., Kobayashi Q S., Jin and Jiang X D. (1996). Fine structure of the acinar and duct cell components in the parotid and submandibular salivary glands of the rat: a TEM, SEM, and HRSEM study. Histol Histopathol 11 : 103-110.

62. Yang YD., Cho H., Koo JY., Tak MH., Cho Y., Shim W., Park SP., Lee J., Lee B., Kim B., Raouf R., Shin YK and Oh U. (2008). TMEM16A confers receptor-activated calcium-dependent chloride conductance Nature volume 455, pages 1210–1215.

63. Zhang G., Li T., Wang H., and Liu J. (2017). The pathogenesis of iodide mumps. Medicine (Baltimore). Nov; 96(47): e8881.